5th ECCOMAS Thematic Conference on
Computational Methods in Structural Dynamics and Earthquake Engineering
M. Papadrakakis, V. Papadopoulos, V. Plevris (eds.)
Crete Island, Greece, 25–27 May 2015

BEHAVIOUR OF NON-CONFORMING R.C. MEMBERS UNDER COMPRESSIVE AXIAL LOAD AND BIAXIAL BENDING

Marta Del Zoppo[1], **Marco Di Ludovico**[2] **and Aurelio Ghersi**[3]

[1] Ph.D. Student, Department of Engineering
University of Naples "Parthenope"
e-mail: marta.delzoppo@uniparthenope.it

[2] Assistant Professor, Department of Structures for Engineering and Architecture
University of Naples "Federico II"
e-mail: diludovi@unina.it

[3] Full Professor, Department of Civil and Environmental Engineering
University of Catania
e-mail: aghersi@dica.unict.it

Keywords: existing building; biaxial bending; ultimate curvature domain; yielding curvature; rotational capacity; chord rotation.

Abstract. *Under seismic actions, the structures undergo two simultaneous horizontal components of the ground motion, which cause a structural response in an oblique direction and biaxial bending in the columns. The current approach to the seismic design of new structures or the assessment of existing ones points out the need of taking into account the contemporaneous presence of the two components of ground motion, in order to make a good prediction of the real structural behaviour, both in terms of strength and deformation capacity. The paper analyses the influence of the two components of bending moment on the deformation capacity of reinforced concrete (r.c.) cross-sections and r.c. members (i.e. columns) by using a specific fibre model. The behaviour of the generic member is expressed in terms of ultimate/yielding curvature domain for the cross-section and ultimate/yielding rotational capacity domain for the column. The study underlines the influence of the two components of biaxial bending on the deformation capacity of r.c. cross-sections and r.c. members.*

1 INTRODUCTION

During a seismic event, the structures are subjected to two simultaneous horizontal components of the ground motion, which cause a structural response in an oblique direction and biaxial bending on the columns.

In XX century, the usual approach for the evaluation of the capacity of structures under seismic excitations was based on the analysis of two unidirectional independent actions. Several experimental researches have been carried out under this simplified hypothesis, assuming the structural elements (i.e. columns) mainly subjected to compressive axial load and uniaxial bending. According to the current seismic codes provisions [1, 2], it is possible to analyse and design the structure assuming two unidirectional independent actions and then combining the results of the two separate analyses. In order to refine the prediction of the structural capacity, both in term of strength and deformation capacity, the contemporaneous presence of the two components of ground motion should be taken into account in structural analysis.

The strength capacity of reinforced concrete (r.c.) cross-sections subjected to compressive axial load and biaxial bending has been widely investigated in literature. The most general approach to the analysis of cross-sections subjected to two components of bending moment is the numerical procedure, which discretizes the cross-section in fibres and integrates the stress distribution over the cross-section area [3, 4, 5, 6]. An alternative and simplified approach is the definition of analytical formulations for the evaluation of the failure surface N-M_x-M_y for a generic r.c. cross-section. The most diffused analytic formulation is the Load Contour method [7], which describes the strength domain M_x-M_y for square/rectangular cross-sections as a function of the uniaxial flexural strength (Eq. 1).

$$\left(\frac{M_{Ed,x}}{M_{Rd,x}}\right)^{\alpha_1}+\left(\frac{M_{Ed,y}}{M_{Rd,y}}\right)^{\alpha 2}\leq 1 \qquad (1)$$

Recently, the attention have been focused on the behaviour of r.c. cross-sections in terms of deformation (i.e. curvature) capacity. Based on the results of numerical analysis, some authors proposed the cross-section failure domain $\phi_{u,x}$-$\phi_{u,y}$ in terms of ultimate curvature achieved before the failure [5, 8]. In [9] a simplified procedure for the evaluation of the ultimate curvature of doubly symmetric r.c. cross-sections is proposed. Nevertheless, general analytical formulations for the ultimate curvature in biaxial conditions are still lacking.

Similarly, a lack of investigation has been found about the deformation (i.e. rotational) capacity of r.c. members subjected to two components of bending moment. Several studies investigated on the experimental evaluation of the chord rotation for r.c. members under uniaxial bending [10, 11, 12, 13]. Analytical formulations for the chord rotation at ultimate conditions under uniaxial bending are provided by codes [1, 14].

Experimental studies on the behaviour of r.c. members subjected to different and oblique loading paths have been proposed in literature by [15, 16, 17, 18].

The experimental results confirm that the biaxial bending action affects the rotational capacity of r.c. members more than their strength and underline the need for numerical and analytical models, which relate biaxial bending and axial load in the evaluation of the deformation capacity of r.c. members.

Some authors performed numerical analyses with specific fibre models extended to the member length [6, 19, 20] in order to evaluate the theoretical rotational capacity of the biaxially loaded members.

The purpose of this study is to show the behaviour of r.c. members under simultaneous compressive axial load and biaxial bending, focusing particular attention on the reduction of deformation capacity due to the two components of bending. The analysis on the generic r.c. member is performed with a specific numerical model, which takes into account the tension shift phenomenon due to the simultaneous presence of shear and bending moment, the deformation of anchorage bars at the joint and the softening branch in the Moment-Curvature diagram.

2 RESEARCH SIGNIFICANCE

The influence of bi-directional seismic excitations on the inelastic behaviour of r.c. members is a crucial aspect to correctly predict the structural behaviour. Taking into account the two components of ground motion, the columns are subjected to combined compressive axial load and biaxial bending, which reduces significantly the deformation capacity of r.c. members. In particular, the study focuses on the behaviour of non-conforming r.c. columns, typical of existing buildings. The present paper proposes curvature domains and chord rotation domains, obtained performing nonlinear analyses with a specific numerical model. The reduction of deformation capacity due to the two components of bending underlines the need of new formulations able to take into account the behaviour of members under biaxial actions.

3 NUMERICAL MODEL FOR THE ANALYSIS OF R.C. MEMBERS

The present research is carried out by using a specific numerical procedure for the evaluation of the nonlinear behaviour of r.c. members under combined axial load and biaxial bending moment [6]. As aforementioned, the behaviour of an r.c. member is strictly related to the behaviour of its cross-section. In a generic r.c. cross-section subjected to axial load N and two components of bending moment M_x-M_y, the inclination angle α_n of the neutral axis n is different from the inclination angle β (Eq. 2) of the bending axis m (Fig. 1a).

$$\beta = \tan^{-1}\frac{M_y}{M_x} \tag{2}$$

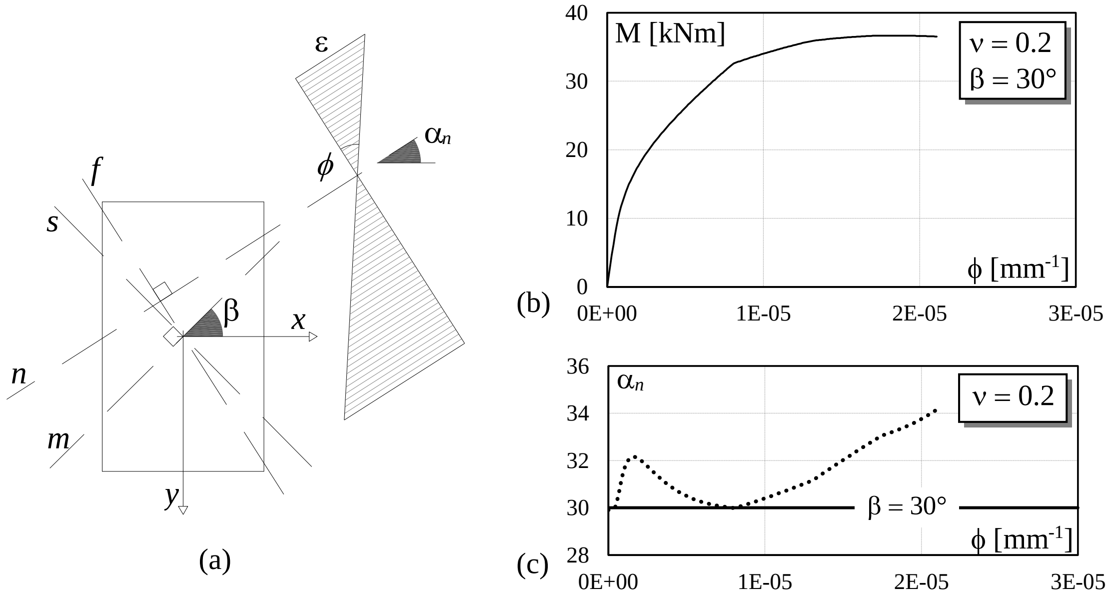

Figure 1: (a) Cross-section under biaxial bending (b) Moment-Curvature relationship for a given β and ν and (c) α_n - ϕ relationship for a given β.

The cross-section curvature ϕ is a function of the neutral axis inclination angle α_n, which in case of biaxial bending could be evaluated only by iterative procedures. Performing a moment-curvature analysis on a generic r.c. cross-section assuming a constant inclination angle β of the bending axis *m* (Fig. 1b), the value of the inclination angle α_n is different from β (Fig. 1c). Moreover, the relation between the two angles α_n and β, which is a function of the value of β and of the normalised axial load ν, is not analytically predictable.

The deflection of three-dimensional members is strictly related to the inclination angle α_n of the neutral axis. In general, the deflection of an r.c. member subjected to biaxial bending is three-dimensional. However if the direction of displacements is imposed, as in conventional pushover analysis, the deflection of the member will be plane along this direction. In other words, if the inclination of the deflection axis *f* (i.e. the inclination angle α_n) is assumed constant during the load history, the deflection of the member is plane.

The adopted numerical procedure performs the analysis of r.c. members for a fixed inclination angle α_n of the neutral axis, in order to guarantee a plane deflection of the generic three-dimensional member. The model replicates an experimental test on an r.c. cantilever subjected to compressive axial load and oblique loading path [18].

The analysis is performed on the cross-section firstly and then on the member. The generic r.c. cross-section is analysed using a specific fibre model. The cross-section is divided in a finite number of triangles and then each triangle is discretized in a finite number of fibres (i.e. strips) parallel to the direction α_n of the neutral axis. At each fibre is assigned a nonlinear constitutive law for concrete. The steel reinforcement properties are assumed to be concentrated at the location of each steel bar. The Moment-Curvature relationship for the generic cross-section is obtained by an iterative procedure with increasing curvature ϕ until the failure. At each step of curvature, the procedure finds the neutral axis depth able to satisfy the equilibrium between external and internal actions.

The generic r.c. member is herein analysed as the basic scheme of cantilever with constant cross-section along its length L_V (i.e. the shear span of the member), subjected to a horizontal force F at the free end. Displacements and rotations for the cantilever are obtained by integration of the curvatures along the member length, including the deformation of steel bars inside the joint. The numerical procedure adopted consists in applying an external curvature ϕ_{fix} at the fixed end of the cantilever. Since the Moment-Curvature relationship for the cross-section is known, the bending moment M_{fix} at the fixed end is easily evaluated, as well as the value of the external force $F=M_{fix}/L_V$ applied at the fixed end.

The diagram of the bending moment along the member length takes into account the tension shift phenomenon, due to the simultaneous presence of bending moment and shear. The *effective bending moment diagram* is obtained shifting the bending diagram of the quantity Δz (Fig. 2a). The consequence of the tension shift is that part of the member near the fixed end is characterized by constant bending moment. The value of curvature in this portion of member is constant and equal to the curvature at the fixed end, so that it behaves as a unique element subjected to the same curvature. Then the wider part of the flexural deformation is here concentrated, so this zone becomes naturally a plastic hinge of length $L_{pl,flex}$ equal to Δz (Eq. 3). The quantity Δz is a function of the internal lever arm z and of the compressive strut inclination angle ϑ, according to the variable strut inclination truss model.

$$L_{pl,\,flex} = \Delta z = 0.5 z \cot \vartheta \tag{3}$$

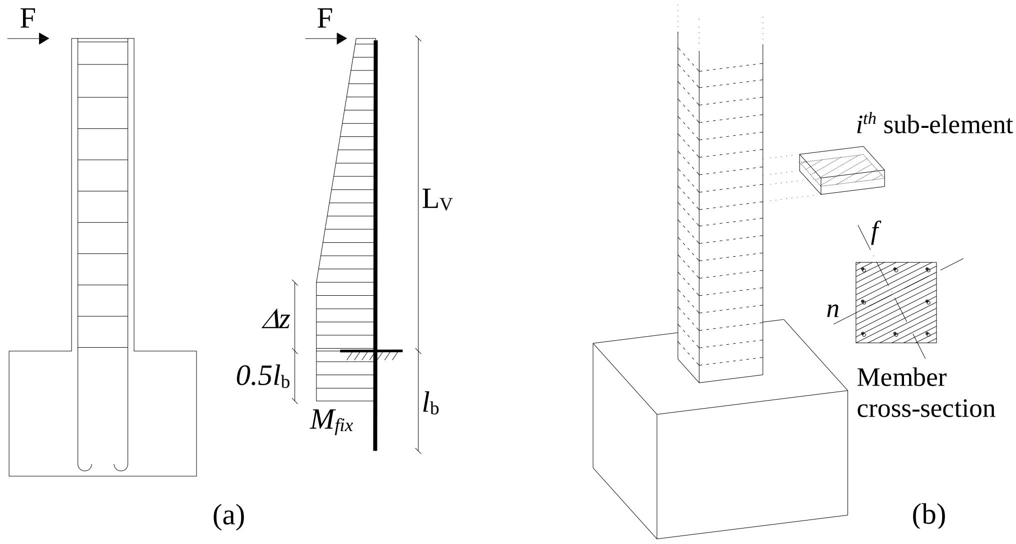

Figure 2: (a) Effective ending moment diagram (b) Cross-section and member discretization

As aforementioned, the model takes also into account the contribution of the tensile reinforcement deformation inside the joint to the rotation of the fixed end. The bending moment is maximum at the fixed end of the cantilever then decreases slowly (it is assumed a linear decreasing) inside the joint becoming null at a distance equal to the steel anchorage length l_b. The bending moment diagram inside the joint could be assumed constant and equal to the bending moment at the fixed end M_{fix}, for a length equal to a half of the anchorage length of steel reinforcement l_b (Fig. 2a). In case of frames, the point of null of bending diagram is at the middle span of the joint, then the bending moment could be considered constant for at least a quarter of the joint global length.

This portion of the joint behaves as a plastic hinge of length $L_{pl,slip}$ equal to a half of the anchorage length of the steel bars l_b (Eq. 4), which is a function of the reinforcement tensile stress σ_s, the bars diameter d_b and the bond stress f_b.

$$L_{pl,\mathrm{slip}} = 0.5 l_b = \frac{\sigma_s d_b}{8 f_b}$$
$$f_b = 2.25 \eta_1 \eta_2 f_{ct} \tag{4}$$

The bond stress f_b is evaluated according to the Eurocode [21], as a function of the concrete tensile strength f_{ct}, reduced by two coefficients η_1 and η_2 which take into account respectively the quality of bond conditions due to smooth/deformed bars and the bars diameter.

The concept of plastic hinge is a natural consequence of the two aforementioned phenomena and the plastic hinge global length L_{pl} is given by the sum of the flexural and slip contributions (Eq. 5). The shear deformation is here neglected.

$$L_{pl} = L_{pl,\mathrm{flex}} + L_{pl,\mathrm{slip}} \tag{5}$$

Once the distribution of bending moment along the cantilever is defined (Fig. 2a), the value of curvature at each section of the cantilever could be evaluated from the cross-section M-ϕ relationship. Herein the cantilever is discretized along its length in a finite number of sub-elements and the curvature is evaluated only at the centroid of each sub-element, in order to reduce the computational effort (Fig 2b). The bending diagram is considered constant along the generic sub-element and the value of bending is assumed equal to the bending moment at its centroid.

The Force-Drift relationship for the member is obtained by iterative procedure with increasing external curvature ϕ_{fix} applied at the fixed end until the failure of the member, due to the achievement of the cross-section ultimate curvature.

4 BEHAVIOUR OF R.C. MEMBERS UNDER BIAXIAL ACTIONS

4.1 Analysis of r.c. cross-section

A sample of the procedure for evaluating the behaviour of r.c. members under biaxial actions is herein explained. In particular, the study focuses on the behaviour of non-conforming r.c. columns, typical of existing buildings.

Two kind of cross-sections are analysed: a square cross-section and a rectangular one. The geometrical percentage of reinforcement, the aspect ratio of the section and the mechanical properties of materials are not significant in this phase since the general trend of the domain curves is analysed independently from these parameters. Nevertheless, the influence of these factors on the reduction of deformation capacity will be evaluated in further studies.

The nonlinear behaviour of concrete is taken into account by adopting the nonlinear stress-strain relationship provided by Eurocode [21], which is a simplification of the model proposed in literature by Sargin [22]. The tensile strength of concrete is neglected so as to the effect of confinement. Then the confined core is assumed to have the same mechanical properties of the unconfined concrete. This assumption is conservative, but is in accordance with the usual hypothesis for existing buildings, in which a lack of stirrups anchorage is always recognized. The mechanical behaviour of reinforcement steel is assumed elastic-perfectly plastic and the contribution of hardening in neglected, as in standard analysis. Moreover, steel bars are considered plain.

The cross-section failure (i.e. the ultimate curvature) corresponds to the achievement of the maximum compressive strain of unconfined concrete $\varepsilon_{cu} = 0.0035$ at the most compressed vertex of the cross-section.

Firstly, the behaviour of the r.c. cross-section subjected to combined compressive axial load and biaxial bending is evaluated by plotting the Moment-Curvature curves for several values of ν. The M-ϕ curves obtained performing the analysis with constant inclination of the neutral axis $\alpha_n = 0°$ (Fig. 3a) show a nonlinear trend with a softening branch for higher values of axial load. In case of softening branch, the ultimate curvature for the cross-section is assumed as the value corresponding to 80% of the maximum bending moment.

The maximum value of resisting bending moment corresponds to a normalized axial load ν equal to 0.4÷0.5, whereas for higher values of ν the bending capacity of the cross-section decreases. However, this reduction is not so alarming in consideration of the fact that the usual range of normalized axial load for columns is about ν = 0.1÷0.5 both for new structures (due to current codes design provisions) and existing structures (as a consequence of typical design old approaches). It is worth noting the influence of the axial stress level on the cross-section ductility under uniaxial bending. The ultimate curvature between the curves at ν = 0.1 and ν = 0.5 decreases significantly.

Assuming a fixed value of ν and several values of α_n, the Moment-Curvature curves show the same global trend and initial stiffness (Fig. 3b). The effect of biaxial bending (i.e. inclination α_n of the neutral axis) affects more the cross-section ultimate curvature than the cross-section strength. Indeed the reduction in terms of resisting bending moment is quite negligible if compared with the reduction in terms of ultimate curvature and ductility.

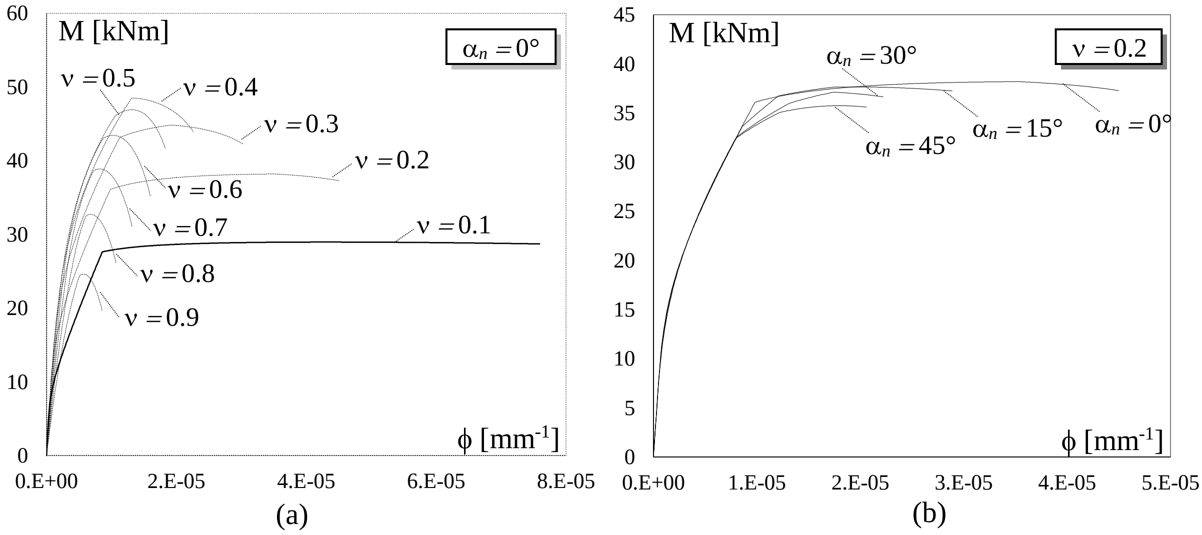

Figure 3: Moment-Curvature curves for different values of (a) ν and (b) α_n.

The cross-section behaviour under biaxial bending is expressed in terms of ultimate curvature domains and yielding curvature domains. The yielding curvature is here evaluated assuming a bilinear curve for the Moment-Curvature relationship, using the approach suggested for the evaluation of the capacity curves by Fajfar [23].

The analysis has been performed on the generic r.c. cross-section, varying the inclination of the neutral axis between $\alpha_n = 0° \div 90°$ and the normalized axial load in the range $\nu = 0.1 \div 0.9$. Starting from the Moment-Curvature curves, the interaction surfaces in terms of yielding curvature and ultimate curvature could be evaluated.

The curvature domain is represented by plotting the two components of yielding/ultimate curvature with respect to the neutral axis inclination angle α_n (Eq. 6)

$$\begin{aligned} \phi_{u(y),x} &= \phi_{u(y)} \cos\alpha_n \\ \phi_{u(y),y} &= \phi_{u(y)} \sin\alpha_n \end{aligned} \tag{6}$$

The ultimate curvature domains have the same global trend for squared and rectangular cross-sections (Fig. 4a-b). Indeed the only difference is the asymmetry of the rectangular cross-section, which is characterized by a lower stiffness along the weak axis, whereas the square section with symmetric reinforcement has the same ultimate curvature under uniaxial bending along the *x*-*y* axis.

The global trend of the curves depends on the normalized axial load, ν. For high values of axial load ($\nu = 0.6 \div 0.9$) the curves are characterized by a concavity faced to the origin of the reference system, whereas for lower values of compressive load ($\nu \leq 0.4$) the concavity of the curves is inverted. Moreover, the trend is approximately linear between $\nu = 0.4 \div 0.5$. It is worth noting that the reduction of ultimate curvature due to the biaxial bending is much relevant for $\nu \leq 0.4$.

In doubly symmetric cross-sections, as the square sections with symmetric reinforcement, the minimum value of the ultimate curvature is always achieved at $\alpha_n = 45°$. This condition is independent from the axial load and depends only from the geometry.

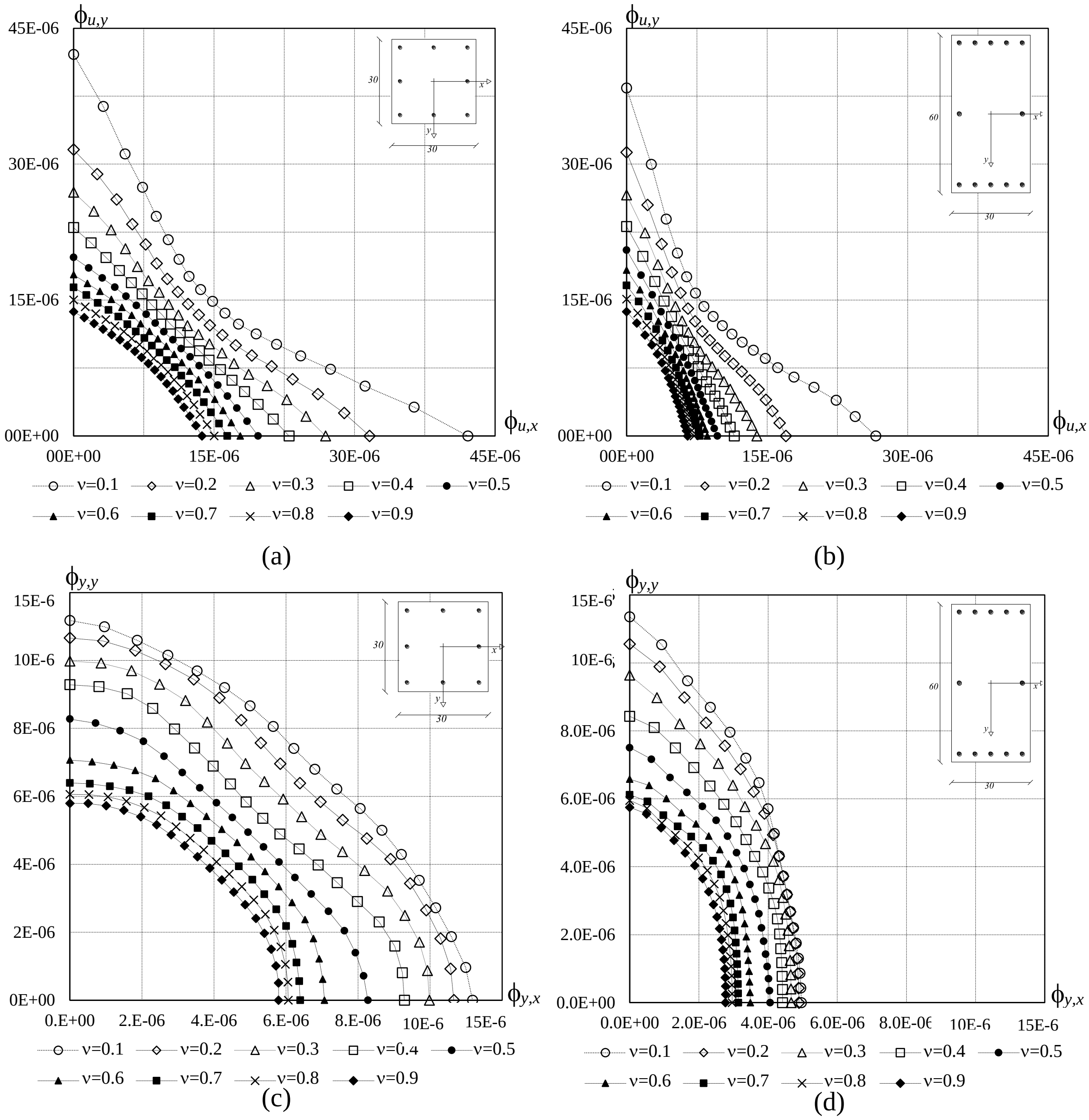

Figure 4: Ultimate curvature domain for (a) square cross-section and (b) rectangular cross-section and yielding curvature domain for (c) square cross-section and (d) rectangular cross-section.

Differently, in case of rectangular cross-sections, the inclination α_n for which the minimum value of ultimate curvature is achieved depends on several factors as the axial load, the cross-section aspect ratio and the location of steel bars. By this, the inclination of neutral axis corresponding to the minimum value of ultimate curvature in case of rectangular cross-section is not predictable.

Similar considerations could be carried out for the yielding curvature. However, the yielding curvature curves (Fig. 4c-d) obtained for square and rectangular cross-sections show the concavity faced to the origin of the reference system, independently from the value of the normalized axial load ν. Moreover, similarly to the case of ultimate curvature, the reduction of yielding curvature due to the axial stress is relevant for low values of ν, whereas for higher values of axial load (ν > 0.5), the reduction is quite negligible.

This is a preliminary step for the evaluation of the redaction of ductility due to the two components of bending moment.

4.2 Analysis of r.c. member

The definition of the Moment-Curvature relationship for the cross-section of the r.c. member is necessary for evaluating the member deflection. As before mentioned, the deflection of an r.c. member subjected to biaxial bending is three-dimensional. Nevertheless, if the two components of bending increase in a way that allow to have a constant inclination angle α_n of the neutral axis (i.e. for a fixed direction of displacement path), the deflection of the member is plane over the plane of deflexion.

The member behaviour under biaxial bending is expressed in terms of ultimate chord rotation domains and yielding chord rotation domains. Analogously to the case of cross-section, the yielding rotation is evaluated assuming a bilinear curve for the Moment-Rotation relationship using the approach suggested for the evaluation of the capacity curves by Fajfar [23].

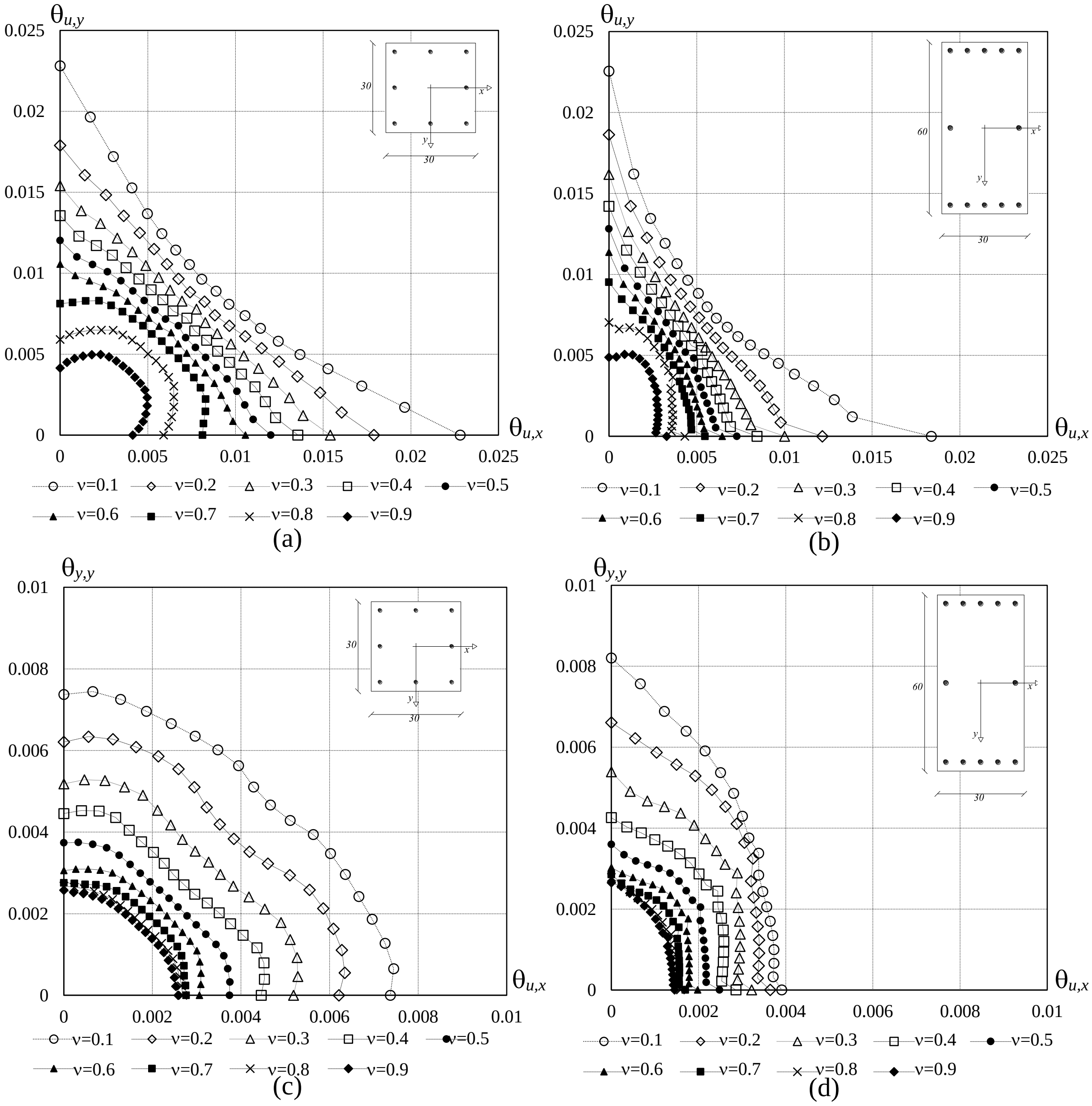

Figure 5: Ultimate rotation domain for (a) squared cross-section and (b) rectangular cross-section and yielding rotation domain for (c) squared cross-section and (d) rectangular cross-section.

The Moment-Rotation relationship is calculated for several inclination of the neutral axis between $\alpha_n = 0° \div 90°$ and varying the normalized axial load in the range $\nu = 0 \div 0.9$. Then the three-dimensional ultimate/yielding chord rotation domain is obtained (Fig. 5).

The general trend of ultimate rotation domain curves is very close to the ultimate curvature domain (Fig. 5a-b). For high values of axial load the concavity of the curves is faced to the origin but the ultimate rotation under biaxial bending is higher than the uniaxial one. It is observed that for values of $\alpha_n \cong 0°$ the failure is caused by achievement of 20% reduction of the strength capacity. For $\nu = 0 \div 0.3$ the concavity is in the opposite direction and the reduction of the capacity due to the biaxial bending is evident.

On the contrary, the concavity of yielding rotation domain curves is always faced to the origin, independently from the entity of ν (Fig. 5c-d). For normalized axial load higher than 0.6 the difference between the curves is negligible.

The representation of the curvature and rotation domains for the generic r.c. member confirms the strong correlation between the behaviour of the member and the behaviour of its cross-section.

5 COMPARISON BETWEEN NUMERICAL RESULTS AND CODE PROVISIONS

The evaluation of the ultimate and yielding rotation of r.c. members is crucial for defining the deformation capacity of existing buildings or new constructions.

The current European code [14] provides a specific formulation for calculating the yielding and ultimate rotation of r.c. member under uniaxial actions. In particular, the expression of the yielding rotation is given by the sum of three contribution: (i) the flexural rotation, (ii) the shear deformation and (iii) the deformation due to the bond slip (Eq. 7). It is a function of the mechanical properties of materials (i.e. steel yielding strength f_y and concrete compressive strength f_c) and geometrical characteristic of the member (i.e. shear span L_V and cross-section depth h)

$$\theta_y = \phi_y \frac{L_V}{3} + 0.0013\left(1 + 1.5\frac{h}{L_V}\right) + 0.13\phi_y \frac{d_b f_y}{\sqrt{f_c}} \tag{7}$$

A critical aspect of this formulation is the accuracy in the evaluation of the yielding curvature ϕ_y for elements subjected to compressive axial load and bending moment. Usually, the yielding curvature is associated to the yielding of tensile reinforcement. Nevertheless, this value of yielding curvature is not representative for sections subjected to compressive axial load and biaxial bending and implies an underestimation of the yielding rotation. A more accurate procedure is the evaluation of the bilinear curve of Moment-Curvature relationship for the cross-section. Therefore, this method requires a higher computational effort and generally is not used in standard applications. For the following examples, the yielding curvature is calculated with a simplified approach, assuming both steel reinforcement yielded.

According to the codes provisions [14, 24], the ultimate chord rotation could be calculated choosing between the two formulations provided (Eq 8a). The first one is an additive formulation where the yielding rotation is increased by the plastic rotation above a reduced plastic hinge. The second expression is based on results of experimental tests [25] and takes into account the effectiveness of confinement α_c, which increases the rotational capacity (Eq 8b).

$$\theta_u = \frac{1}{\gamma_{el}}\left(\theta_y + (\phi_u - \phi_y)L_{pl}\left(1 - \frac{0.5L_{pl}}{L_V}\right)\right)$$
$$\theta_u = \frac{1}{\gamma_{el}}0.016\left(0.3\right)^{\nu}\left[\frac{\max\left(0.01;\omega'\right)}{\max\left(0.01;\omega\right)}f_c\right]^{0.225}\left(\frac{L_V}{h}\right)^{0.35}25^{\left(\alpha_c\rho\frac{f_{yw}}{f_c}\right)}\left(1.25^{100\rho_d}\right) \tag{8}$$

In case of members characterized by ties not closed with 90-degree hooks at both ends, the code suggests to neglect the effectiveness of confinement, assuming $\alpha_c = 0$ in the second expression. Moreover, in case of elements without seismic details, the ultimate rotation is 85% of the value obtained previously assuming $\alpha_c = 0$.

The results provided by the numerical procedure herein described are here compared with the results of codes formulations under uniaxial bending (Fig. 6a). For values of normalized axial load $\nu \leq 0.5$, the trend of the numerical results under uniaxial bending (i.e. $\alpha_n = 0°$) is very close to the results of (Eq. 8a). In case of biaxial bending (i.e. $\alpha_n = 45°$), the ultimate rotation is strongly reduced in case of low normalized axial loads. The codes formulations, (Eq. 8a) and (Eq. 8b), provide different results. In particular, the (Eq. 8a) provides results more conservative than (Eq. 8b), even though the reductions applied at (Eq. 8b) in case of non-conforming elements. Nevertheless, also (Eq. 8a) overestimates the rotational capacity, if the effect of biaxial bending is considered.

Moreover, for higher values of ν, the strong compressive stress reduces significantly the rotational capacity, but the (Eq. 8a) is not able to catch this phenomenon, in part due to the approximation in the evaluation of the yielding rotation and in part due to the evaluation of the plastic hinge length.

The plastic hinge length L_{pl} is calculated according to the equation provided by [14] Eq. 9). In particular, the global plastic hinge length is given by the sum of three contributions (Fig. 6b): (i) the flexural contribution $L_{pl,flex}$, (ii) the shear contribution $L_{pl,shear}$ and (iii) the bond slip contribution $L_{pl,slip}$.

$$L_{pl} = 0.1L_V + 0.17h + 0.24\frac{d_b f_y}{\sqrt{f_c}} \tag{9}$$

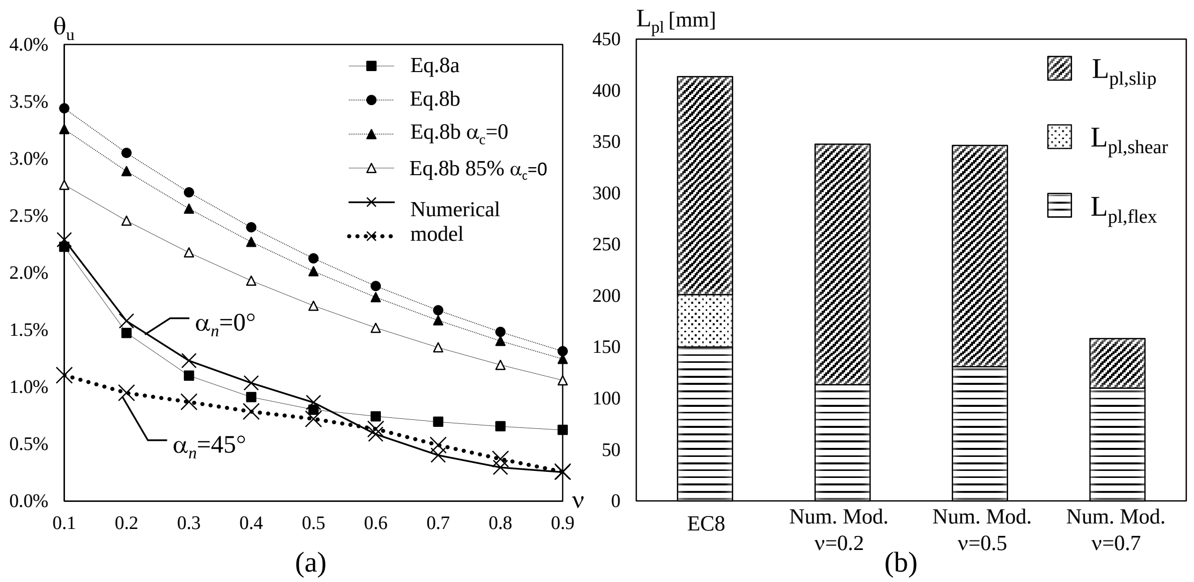

Figure 6: (a) Comparison between codes provisions and numerical model results in uniaxial conditions (b) Comparison of plastic hinge length calculated with EC8 formulation and with the numerical model.

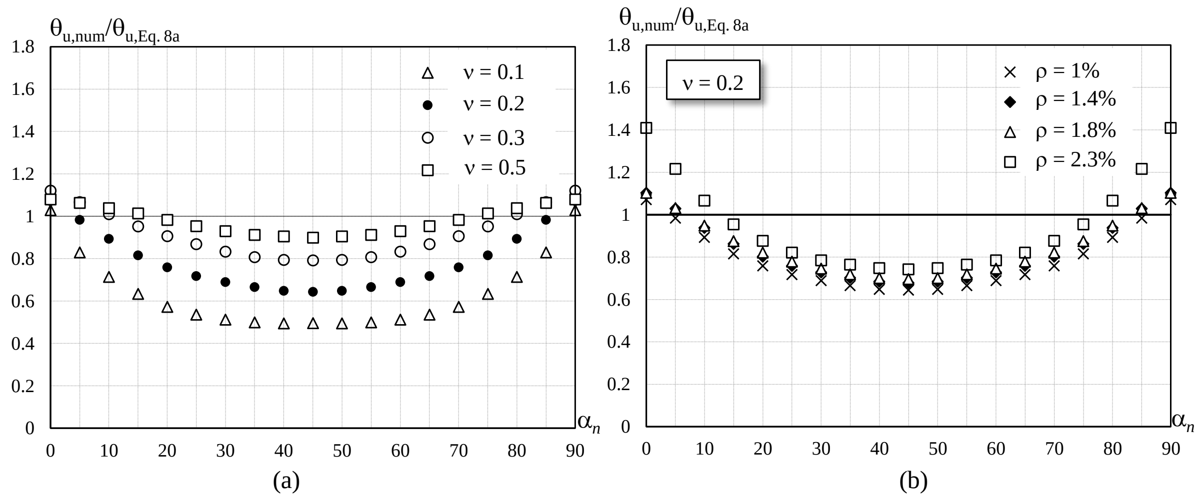

Figure 7: (a) Comparison between codes provisions and numerical results under biaxial actions for several ν and (b) Comparison between codes provisions and numerical results under biaxial actions for several ρ.

The numerical model is able to catch both the flexural and anchorage bars contributions. The shear deformation, neglected in the model, is smaller than the other two contributions. Moreover, the effect of the compressive axial load reduces the plastic hinge length (in particular the component due to the deformation of reinforcement in tension inside the joint), but the formulation provided by the code is independent from ν.

The ratio between the ultimate rotation capacity computed by the numerical procedure and that provided by (Eq. 8a) for uniaxial bending is plotted as a function of α_n in (Fig. 7a). The Figure shows that, if biaxial action are neglected, the capacity of the cross-section is overestimated. Moreover, the reduction of ultimate rotation is stronger for low values of axial load, arriving at 50% of the uniaxial ultimate rotation.

In conclusion, the axial load strongly affects the trend of the deformation capacity curves. Nevertheless, other parameters, like the geometric percentage of reinforcement (Fig. 7b) or the mechanical properties influence the reduction due to the biaxial bending. The analysis of such influence is outside the scope of the present research, but will be the goal of further studies.

6 CONCLUSIONS

The deformation capacity of r.c. members subjected to compressive axial load and biaxial bending has been evaluated using a specific numerical procedure. Firstly, the yielding and ultimate curvature domains for the r.c. cross-section of non-conforming elements have been evaluated and discussed. Then, the yielding and ultimate rotation domains for the r.c. member have been plotted, taking into account the nonlinear behaviour of concrete, the softening branch of the Moment-Curvature relationship, the tension shift phenomenon and the deformation of anchorage bars.

The results of the numerical analyses confirm the reduction of deformation capacity due the two components of bending, in terms of both ultimate curvature and rotational capacity. In particular, the reduction is stronger in the range of normalized axial load value $0.1 \leq \nu \leq 0.5$, typical of columns.

The expressions provided by the Eurocode 8 [14] for the evaluation of the ultimate rotation under uniaxial actions provide different results. In particular, the additive formulation (Eq. 8b) is particularly conservative but it is also widely used in standard applications. The results of the numerical procedure under uniaxial bending have a good agreement with the (Eq. 8a) for normalized axial load lower than 0.6.

Moreover, assuming the rotational capacity of the member constant for each direction and equal to the uniaxial one, estimated by (Eq. 8a), the ultimate rotation under biaxial actions in the examined cases is overestimated up to 50%.

This research underlines the need of further investigation on the behaviour of non-conforming r.c. member subjected to biaxial bending, in order to provide new formulations able to easily and reliably predict the rotation capacity in biaxial conditions.

REFERENCES

[1] ASCE, Seismic rehabilitation of existing buildings, *ASCE SEI/41*, *ASCE, Reston, VA*, 2007.

[2] European Standard, Eurocode 8: Design of structures for earthquake resistance. Part 1: General rules, seismic actions and rules for buildings, *EN 1998-1*, Brusselles, Belgium, 2003.

[3] M. G. Sfakianakis, Biaxial Bending with Axial Force of Reinforced, Composite and Repaired Concrete Section of Arbitrary Shape by Fiber Model and Computer Graphics, *Advanced in Engineering Software*, **33**, 227-242, 2002.

[4] M. Di Ludovico, G. P. Lignola, A. Prota, E. Cosenza, Nonlinear analysis of cross-sections under axial load and biaxial bending, *ACI Structural Journal*, **107**(4), 390-399, 2010.

[5] M. Fossetti, M. Papia, Dimensionless analysis of RC rectangular sections under axial load and biaxial bending, *Engineering Structures*, **44**, 34-45, 2012.

[6] M. Bosco, M. Del Zoppo, A. Ghersi, E. M. Marino, A model for the analysis of reinforced concrete cross-sections and members under biaxial bending and axial force, *proposed to Computers and Structures*, 2015.

[7] B. Bresler, Design criteria of reinforced columns under axial load and biaxial bending, *ACI Journal*, **57**(5), 481-490, 1960.

[8] M. Di Ludovico, G. P. Lignola, A. Prota, E. Cosenza, Analisi non lineare di sezioni in c.a. soggette a pressoflessione deviata, *ANIDIS XII Convegno*, *L'Ingegneria sismica in Italia*, Pisa, Italy, 2007.

[9] M. Di Ludovico, G. M. Verderame, I. Iovinella, E. Cosenza, Domini di curvatura di sezioni in c.a. in pressoflessione deviata. Parte II, *ReLuis Convegno*, Rome, Italy, 2008.

[10] M. N. Fardis, D. E. Biskinis, Deformation capacity of RC members, as controlled by flexure or shear, *Performance based engineering for earthquake resistant reinforced concrete structures: A volume honoring Shunsuke Otani, T. Kabeyasawa and H. Shiohara, eds.*, University of Tokyo, Tokyo, 511–530, 2003.

[11] M. Berry, M. Eberhard, Performance models for flexural damage in reinforced concrete columns, *Rep. No. 2003/18*, PEER Center, University of California, Berkeley, CA, 2003.

[12] M. Eberhard, *Structural Performance Database*, Dept. of Civil and Environmental Engineering, Univ. of Washington, *http://www.ce.washington.edu/peera1/last*, 2005.

[13] M. Di Ludovico, G. M. Verderame, A. Prota, G. Manfredi, E. Cosenza, Cyclic behavior of nonconforming full-scale RC columns, *J. Struct. Eng.*, **140**(5), 2014.

[14] European Standard, Eurocode 8: Design of structures for earthquake resistance. Part 3: Assessment and retrofitting of buildings, *EN 1998-3*, Brusselles, Belgium, 2004.

[15] S. N. Bousias, G. Verzeletti, M. N. Fardis, M., E. Gutierrez, Load path effects in column biaxial bending with axial force, *J. Eng. Mech.*,**121**(5), 596–605, 1995.

[16] F. Qiu, W. Li, P. Pan, L. Qian, Experimental tests on reinforced concrete columns under biaxial quasi-static loading, *J. Eng. Struct.*, 24(4), 419–428, 2002.

[17] H. Rodrigues, A. Arede, H. Varum, A. G. Costa, Experimental evaluation of rectangular concrete column behaviour under biaxial cyclic loading, *Earthquake Engng Struct. Dyn.*, **42**, 239-259, 2013.

[18] M. Di Ludovico, G. M. Verderame, A. Prota, G. Manfredi, E. Cosenza, Experimental behaviour of nonconforming RC columns with plain bars under constant axial load and biaxial bending, *J. Struct. Eng.*, **139**, 897-914, 2013.

[19] C. A. Christos, S. A. Mahin, Behavior of reinforced concrete structures subjected to biaxial excitation, *J. Struct. Eng.*, **117**, 2657-2673, 1991

[20] G.G. Wang, C. T. Hsu, Complete biaxial load-deformation behaviour of RC columns, *J. Struct. Eng.*, 118:2590-2609, 1992.

[21] European Standard, Eurocode 2: Design of concrete structures. Part 1-1: General rules and rules for buildings, *EN 1992-1-1*, Brussels, Belgium, 2004.

[22] M. Sargin, Stress-Strain Relationships for Concrete and the Analysis of Structural Concrete Sections, *SM Study 4, Solid Mechanic Division*, University of Waterloo, 1971.

[23] P. Fajfar, M.EERI, A nonlinear analysis method for performance-based seismic design, *Earthquake Spectra*, **16**(3), 573-592, 2000.

[24] D. M. 14 Gen. 2008, Norme tecniche per il calcolo, l'esecuzione, ed il collaudo delle strutture in conglomerato cementizio armato normale e precompresso e per le strutture metalliche [*Technical guidelines for the design and contruction of reinforced concrete, prestressed concrete and steel structures*], 2008 (in Italian).

[25] T. B. Panagiotakos, M. N. Fardis, Deformations of Reinforced Concrete Members at Yielding and Ultimate, *ACI Structural Journal*, **98**(2), 135-148, 2001.